

An Analytical Investigation for Combined Pressure-Driven and Electroosmotic Flow Without the Debye–Huckel Approximation



Avisankha Dutta and Sudip Simlandi

Abstract In the present work, an analytical solution is presented for a combined pressure-driven electroosmotic flow of a Newtonian liquid within a microchannel between two parallel plates. The electroosmotic flow is considered to be induced by an externally applied electrostatic potential field and a pressure gradient. The no-slip boundary conditions are considered. The electric potential distribution is represented by the Poisson–Boltzmann equation. The Debye–Huckel linear approximation is ignored in the present work to minimize error in results. The reduced form of the Navier–Stokes and the energy equations are considered, respectively, to determine velocity and temperature distributions. Homotopy perturbation method (HPM) is adopted as an analytical tool to solve the nonlinear Poisson–Boltzmann equation for electrical potential distribution without the Debye–Huckel linear approximation. The Navier–Stokes and the energy equations subjected to respective boundary conditions are solved analytically. An expression of $C_f Re$ product is obtained solving the Navier–Stokes equation. The results obtained are validated with existing literature and show good agreement. The zeta potential is varied for a particular electrokinetic length, and proposed results are presented graphically. Finally, the Nusselt number is presented varying electrokinetic length for different values of zeta potential. The results demonstrate the influence of the zeta potential on the potential, velocity, temperature distributions, and Nusselt number.

1 Introduction

In recent days, the study on microfluidic systems has become an important area of research for various potential applications in biomedical and chemical industry. Biomedical microelectromechanical systems or bioMEMS can accomplish sample

A. Dutta · S. Simlandi (✉)

Department of Mechanical Engineering, Jadavpur University, Kolkata 700032, India
e-mail: sudip.simlandi@gmail.com

A. Dutta

e-mail: avisankha@gmail.com

© Springer Nature Singapore Pte Ltd. 2020

A. N. R. Reddy et al. (eds.), *Intelligent Manufacturing and Energy Sustainability*,
Smart Innovation, Systems and Technologies 169,
https://doi.org/10.1007/978-981-15-1616-0_54

553

injection, chemical reaction, separation, and detection in a single integrated microfluidic circuit [1]. Various techniques such as thermopneumatic, magnetohydrodynamic, piezoelectric, electrostatic, and electroosmotic pumping have been proposed for fluid delivery. Among these, the electroosmotic pumping is preferred because pumping a liquid through a very small channel requires a very large pressure difference, whereas it does not require any external pump, but needs electrodes to control the flow field. Due to the absence of moving parts and pulsating flows, ease of microfabrication, and a great degree of flow control, the electroosmotic pumping is very popular [2–6]. Therefore, it is important to understand the fundamental characteristics of electroosmotic flow (EOF) through microchannels for optimal design and efficient control and to ensure the reliability and the stability of the microfluidic devices of electroosmotic pumps. When an electrolytic solution is under no flow condition, the ions dissociate. Those ions having charge opposite to that of the surface are attracted by the surface. Thus, two layers of positively and negatively charged ions are formed near the surface which are called electric double layer (EDL). If a pressure gradient and an electric field are applied tangentially along such a charged surface, the ions in the diffuse layer will start moving under the action of the pressure field and body force exerted by the electric field, resulting in pressure-driven EOF [3].

In this connection, few literatures are studied. Masood Khan et al. [5] discussed the dynamics of an EOF in cylindrical domain. The linearized Poisson–Boltzmann equation and the Cauchy momentum equation were solved using the temporal Fourier and finite Hankel transforms. Ngoma and Erchiqui [7] investigated the liquid flow with the slip boundary condition in a microchannel between two parallel plates with imposed heat flux. They considered the combined effect of pressure-driven flow and electroosmosis. Jain and Jensen [8] presented an analytical investigation on the effects of electrostatic potential in microchannels. The energy equation was solved with the Nusselt number for constant wall heat flux and constant wall temperature boundary conditions and presented with analytic expressions over a wide range of operating conditions. Min et al. [9] analytically solved the fundamental characteristics of electroosmotic flow through rectangular pumping channels without the Debye–Huckel approximation. The Poisson–Boltzmann equation for the electric potential distribution and the momentum equation for the velocity profile are solved by averaging method. The zeta potential is experimentally measured by the streaming potential technique. They found that their method is applicable when the ratio of a half of the channel width to the EDL thickness is larger than 3.

It is observed from the above literature that conventionally, the electric potential distribution inside a microchannel is determined by a simplified analysis based on the Debye–Huckel linear approximation which is valid for small value of wall zeta potential (usually <25 mV). However, higher range of zeta potentials (100–200 mV) are frequently encountered in practical applications [9–11]. As a result, the accuracy level of the result may reduce. On the other hand, the analytical methods applied are complex, lengthy, and laborious. Hence, it is highly desirable to adopt a simple analytical method to study the fundamental characteristics of EOF through microchannels without the Debye–Huckel approximation. Hence, in the present work, homotopy

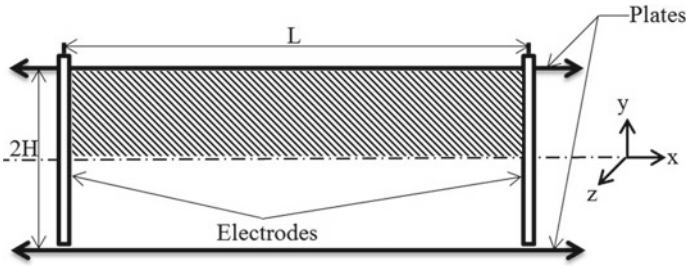


Fig. 1 Geometry of parallel plate microchannel

perturbation method (HPM) as an analytical tool is considered to solve the Poisson–Boltzmann equation as it is a simple, powerful, and efficient solving technique, whereas the Navier–Stokes and the energy equations are also solved analytically for determination of velocity and temperature distributions, respectively, for flow within a microchannel between two parallel plates.

2 Description of the Physical Problem

In the present work, a microchannel consisting of two parallel plates separated by a distance $2H$ is considered as shown in Fig. 1. The plate extends to infinity in x - and z -directions. So, property variation is considered in the y -direction. Because of the symmetry in the potential and velocity fields, the solution domain is reduced to a half section of the channel (as shown by the hatched area in Fig. 1). Two plate-type electrodes are placed apart by length L normal to the parallel plates such that an electric field is induced in the x -direction. A constant pressure gradient is also imposed in the x -direction to study combined effect of both the fields. The following assumptions are made for the mathematical formulation.

- The liquid is a symmetric electrolyte, incompressible, Newtonian and the thermophysical properties are constant.
- The flow is steady, laminar, and fully developed.
- No-slip boundary condition and no wall temperature jump.

3 Mathematical Formulation

In the present study, a combined pressure-driven electroosmotic flow through a microchannel between two parallel plates is considered. The subsequent governing equations subjected to the respective boundary conditions are considered.

3.1 Poisson–Boltzmann Equation

The one-dimensional EDL field can be described by the Poisson–Boltzmann equation given as [8, 10, 12–14]

$$\partial^2\psi/\partial y^2 = (2zen_0/\varepsilon) \sinh(ze\psi/k_bT) \quad (1)$$

where ψ , z , e , n_0 , ε , k_b , and T are the electric potential due to EDL, valence of ions, electric charge, bulk ionic concentration, permittivity of vacuum, Boltzmann constant, and absolute temperature, respectively.

Equation (1) is subjected to the following boundary conditions at $y = 0$, $\partial\psi/\partial y = 0$ and at $y = H$, $\psi =$ wall zeta potential (ξ).

3.2 Momentum Equation

The Navier–Stokes equation [8, 10] along the x -axis is considered by a balance between the shear stresses in the fluid, externally imposed constant pressure gradient, and electric field as

$$\mu(\partial^2u/\partial y^2) - \partial P/\partial x + \rho_f E_x = 0 \quad (2)$$

where μ , u , $\partial P/\partial x$, ρ_f , and E_x are the dynamic viscosity, velocity in x -direction, pressure gradient in x -direction, local net charge density, and the electric field strength, respectively.

The above equation is subjected to the following boundary conditions at $y = 0$, $\partial u/\partial y = 0$ and at $y = H$, $u = 0$.

3.3 Energy Equation

The steady-state energy equation is given as [8, 10, 12–14]

$$u(\partial T/\partial x) = \alpha(\partial^2T/\partial y^2) \quad (3)$$

where $\alpha = \rho C_p/\mu$ is thermal diffusivity.

The boundary conditions are given as at $y = 0$, $\partial T/\partial y = 0$ and at $y = H$, where T is surface temperature.

4 Solution of the Governing Equations

The governing equations for electrical potential, velocity, and temperature distributions have been solved analytically.

4.1 Electric Potential Distribution

The governing Eq. (1) for electrical potential distribution has been solved by homotopy perturbation method (HPM). Equation (1) and its boundary conditions are non-dimensionalized by introducing the dimensionless variables as

$$Y = y/H, \Psi = ze\psi/(k_bT), Z = 2ze\xi/(k_bT)$$

The non-dimensional form of Eq. (1) becomes

$$\partial^2\Psi/\partial Y^2 = \lambda^2 \sinh \Psi \tag{4}$$

where $\lambda = \kappa H$ is the electrokinetic length and $\kappa = \sqrt{[2z^2e^2n_0/(\epsilon k_bT)]}$ is the inverse Debye–Huckel length.

The corresponding non-dimensional boundary conditions are written as at $Y = 0$, $\partial\Psi/\partial Y = 0$ and at $Y = 1$, $\Psi = Z$.

In most of the existing work, the Debye–Huckel approximation is considered where $\sinh \Psi$ in Eq. (4) is replaced by only Ψ . It is already stated that this approximation holds good for small value of zeta potential. In the present study, the Debye–Huckel approximation is ignored to improve the accuracy level of results and to predict results for high range of zeta potential. Hence, in Eq. (4) instead of Ψ , $\sinh \Psi$ is considered. Hence, $\sinh \Psi$ is expanded based on the Taylor series of expansion as

$$\sinh \Psi = \Psi + \Psi^3/3! + \dots \tag{5}$$

Substituting the above relation in Eq. (4) results in

$$\partial^2\Psi/\partial Y^2 = \lambda^2(\Psi + \Psi^3/3! + \dots) \tag{6}$$

The homotopy considered is

$$\Psi'' - \omega^2\Psi + p[(\lambda^2 - \omega^2)\Psi + \lambda^2\Psi^2/3] = 0 \tag{7}$$

where $\Psi'' = \partial^2\Psi/\partial Y^2$, ω is a modified inverse Debye length, and $p \in [0, 1]$ is an embedding parameter, a small parameter in the homotopy perturbation method.

The power series in p used to find the solution of Eq. (7) is

$$\Psi = \Psi_0 + p\Psi_1 + \dots \tag{8}$$

Substituting the above expression in Eq. (7) and arranging the coefficients of p powers, the following homotopy is obtained

$$p^0(\Psi_0'' - \omega^2\Psi_0) + p^1[\Psi_1'' - \omega^2\Psi_1 - (\lambda^2 - \omega^2)\Psi_0 - \lambda^2\Psi_0^3/3!] = 0 \tag{9}$$

Equating the coefficients of p^0, p^1 to zero gives

$$p^0 : \Psi_0'' - \omega^2\Psi_0 = 0 \tag{10}$$

$$p^1 : \Psi_1'' - \omega^2\Psi_1 - (\lambda^2 - \omega^2)\Psi_0 - \lambda^2\Psi_0^3/3! = 0 \tag{11}$$

Equation (10) is solved using the boundary conditions

$$\Psi_0(1) = Z, \Psi_0'(0) = 0$$

and the resulting equation is

$$\Psi_0 = Z \cosh(\omega Y) / \cosh(\omega) \tag{12}$$

Substituting the above expression in Eq. (11) and simplifying the equation give

$$\begin{aligned} &\Psi_1'' - \omega^2\Psi_1 - (\lambda^2 - \omega^2)Z \cosh(\omega Y) / \cosh \omega \\ &- \lambda^2 Z^3 [3 \cosh(\omega Y) + \cosh(3\omega Y)] / [24 \cosh^3 \omega] = 0 \end{aligned} \tag{13}$$

In order to eliminate $\cosh(\omega Y)$ from Eq. (13), the coefficients are collected and equated to zero to predict the value of ω . Equation (13) becomes

$$\Psi_1'' - \omega^2\Psi_1 - \lambda^2 Z^3 \cosh(3\omega Y) / [24 \cosh^3(\omega)] = 0 \tag{14}$$

Now applying the boundary conditions

$$\Psi_1(1) = 0, \Psi_1'(0) = 0$$

Eq. (14) is solved as

$$\Psi_1 = [\lambda^2 Z^3 / 192 \omega^2 \cosh^3(\omega)] [\cosh(3\omega Y) - \cosh(3\omega) \cosh(\omega Y) / \cosh(\omega)] \tag{15}$$

Substituting the results of Eq. (12) and Eq. (15) in Eq. (8) and considering $p = 1$, the electric potential distribution is obtained as

$$\Psi = A_1 \cosh(\omega Y) + A_2 \cosh(3\omega Y) \tag{16}$$

where $A_1 = Z / \cosh \omega - \lambda^2 Z^3 \cosh 3\omega / [192\omega^2 \cosh^4 \omega]$ and $A_2 = \lambda^2 Z^3 / [192\omega^2 \cosh^3 \omega]$

4.2 Velocity Distribution

The Navier–Stokes equation becomes (18)

$$\mu(\partial^2 u / \partial y^2) = \partial P / \partial x + (2zen_0 / \lambda^2) E_x \partial^2 \Psi / \partial Y^2 \tag{17}$$

where $\rho_f = -2zen_0 \sinh \Psi$ and $\sinh \Psi = (\partial^2 \Psi / \partial Y^2) / \lambda^2$.

Equation (17) is non-dimensionalized incorporating the following non-dimensional terms

$$U = u / u_m, \Gamma_1 = -(H^2 / \mu u_m) \partial P / \partial x, E = E_x L / \xi, \Gamma_2 = 2zen_0 \xi H^2 / (\mu u_0 L)$$

where u_m is the mean velocity.

Hence, the Eq. (17) for the velocity field is written as

$$\partial^2 U / \partial Y^2 = -\Gamma_1 + (\Gamma_2 E / \lambda^2) (\partial^2 \Psi / \partial Y^2) \tag{18}$$

The corresponding non-dimensional boundary conditions become at $Y = 0$, $\partial U / \partial Y = 0$ and at $Y = 1$, $U = 0$.

Finally, the velocity profile is obtained by integrating Eq. (18) twice with respect to Y with the given boundary conditions as

$$U = \Gamma_1 (1 - Y^2) / 2 + (\Gamma_2 E Z / \lambda^2) [(A_1 \cosh(\omega Y) + A_2 \cosh(3\omega Y)) / Z - 1] \tag{19}$$

The relation between Γ_1 and Γ_2 is determined from the definition of mean velocity as

$$\int_0^1 U dY = 1 \tag{20}$$

and obtained as

$$\Gamma_2 = (\lambda^2 / EZ) (1 - \Gamma_1 / 3) / [(A_1 \sinh(\omega) / (\omega) + A_2 \sinh(3\omega) / (3\omega)) / Z - 1] \tag{21}$$

Now, the skin friction coefficient C_f is defined as [8]

$$C_f = 2\tau_w / (\rho U^2) \tag{22}$$

The product $C_f Re$ is obtained as

$$C_f Re = 8U'(1) \quad (23)$$

where $Re = \rho u_m(4H)/\mu$ is the Reynolds number.

4.3 Temperature Distribution

Equation (3) for temperature field is simplified by performing scale analysis as

$$\dot{q}'' \sim (\dot{m}c_p \Delta T/A) \sim \rho c_p u_m \Delta T \text{ and } \dot{q}'' \sim h(T_m - T_s)$$

where \dot{q}'' , \dot{m} , C_p , ΔT , A , ρ , h , and T_m are the wall heat flux, mass flow rate of liquid, specific heat, temperature scale, area normal to heat flow, convective heat transfer coefficient, and mean temperature, respectively.

From the above relations, it is observed that

$$\partial T/\partial x = \Delta T/\Delta x = \dot{q}''/(\rho u_m c_p H) \quad (24)$$

where Δx is the length scale in x -direction.

Combining Eqs. (3) and (24), the relation obtained is as follows

$$\partial^2 T/\partial y^2 = u\dot{q}''/(\alpha \rho u_m c_p H) \quad (25)$$

Equation (25) is non-dimensionalized considering

$$\Phi = (T - T_s)/(T_m - T_s) \text{ and } Nu = (4H)(h)/K$$

and is written as

$$\partial^2 \Phi/\partial Y^2 = (Nu)(U)/4 \quad (26)$$

The corresponding boundary conditions become at $Y = 0$, $\partial \Phi/\partial Y = 0$ and at $Y = 1$, $\Phi = 0$.

Substituting the expression (Eq. (19)) for velocity distribution in Eq. (26) gives

$$\begin{aligned} \partial^2 \Phi/\partial Y^2 = (Nu/4)[\Gamma_1(1 - Y^2)/2 + (\Gamma_2 EZ/\lambda^2) \\ \{[A_1 \cosh(\omega Y) + A_2 \cosh(3\omega Y)]/Z - 1\}] \end{aligned} \quad (27)$$

Thereafter, the Eq. (27) is integrated twice with respect to Y with the given boundary conditions to yield the temperature distribution as follows:

$$\begin{aligned} \Phi = (Nu/4)[\Gamma_1(Y^2/4 - Y^4/24 - 5/24) + (\Gamma_2 EZ/\lambda^2)[\{9A_1 \cosh(\omega Y) - 9A_1 \cosh(\omega) \\ + A_2 \cosh(3\omega Y) - A_2 \cosh(3\omega)\}/(9Z\omega^2) + (1 - Y^2)/2]] \end{aligned} \quad (28)$$

The mean temperature is defined as

$$\int_0^1 U \Phi dY = 1 \tag{29}$$

Finally, the expression of Nusselt number, Nu, is determined at the wall by substituting Eqs. (19) and (28) in the Eq. (29) and written as

$$Nu = 4 / \int_0^1 \Gamma_1(1 - Y^2)/2 + (\Gamma_2 EZ/\lambda^2) [\{A_1 \cosh(\omega Y) + A_2 \cosh(3\omega Y)\}/Z - 1] [\Gamma_1(Y^2/4 - Y^4/24 - 5/24) + (\Gamma_2 EZ/\lambda^2) \{9A_1 \cosh(\omega Y) - 9A_1 \cosh(\omega) + A_2 \cosh(3\omega Y) - A_2 \cosh(3\omega)\} / (9Z\omega^2) + (1 - Y^2)/2] dY \tag{30}$$

5 Results and Discussion

Finally, a MATLAB program is developed to solve the governing equation. The result obtained is presented in a comparative way with numerical method (FDM) and existing result to check the accuracy level of the proposed work.

In Fig. 2a, b, the potential distributions in the Y-direction for an electrokinetic length of 10 are presented at zeta potential values of 1 and 3, respectively. It is observed that the proposed result is in close agreement with the numerical solution for both the zeta potential values of 1 and 3. For smaller value of zeta potential (i.e., Z = 1), the solution based on the Debye–Huckel approximation agrees well with the numerical solution as shown in Fig. 2a whereas deviates more in Fig. 2b for Z = 3. Hence, the proposed method can be used for a large range of zeta potential.

The velocity distribution obtained for the combined pressure-driven electroosmotic flow is compared with the existing work by Jain and Jansen [8] and numerical results in Fig. 3a, b. The proposed results show close agreement with the numerical

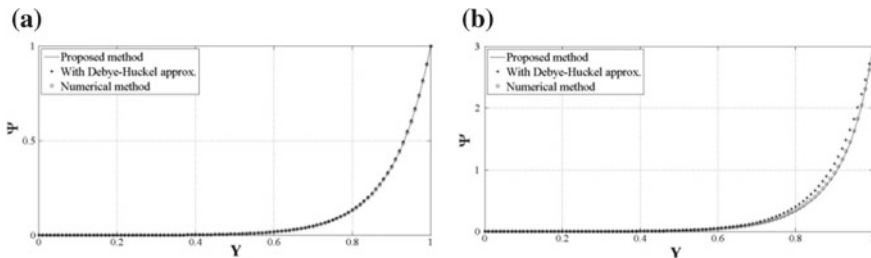


Fig. 2 Non-dimensional potential distribution a Z = 1 and b Z = 3 for λ = 10

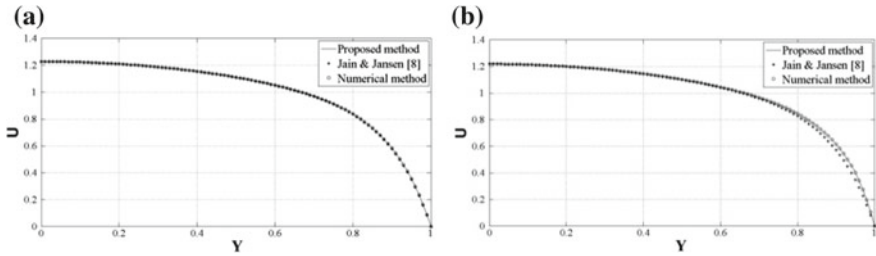


Fig. 3 Non-dimensional velocity distribution **a** $Z = 1$ and **b** $Z = 3$ for $\lambda = 10$

method for $Z = 1$ and 3, whereas the existing work shows a little deviation from the numerical method close to the plate surface for $Z = 3$ as shown in Fig. 3b. This deviation may be due to the effect of the Debye–Huckel approximation considered in the existing work. Hence, the proposed results can predict the velocity distribution for higher values of zeta potential.

Figure 4a, b represents the temperature distribution for an electrokinetic length of 10 and zeta potential values of 1 and 3. Here the solution based on the proposed method is compared with the existing work by Jain and Jansen [8] and numerical results. It is observed that the proposed result is in close agreement with the numerical result for both the zeta potential values of 1 and 3. As a consequence of considering the Debye–Huckel approximation in the existing work, it shows a little deviation from the numerical result close to the plate surface for $Z = 3$ as shown in Fig. 4b. Hence, the proposed method can predict the temperature distribution for higher values of zeta potential.

In Fig. 5a, b, the product $C_f Re$ and the Nu are presented, respectively, as functions of λ for $Z = 1, 2,$ and 3. It is seen that for a particular value of Z the value of $C_f Re$ decreases with increase in λ . It has also been observed for a value of λ , the $C_f Re$ product increases with rise in Z values. This can be attributed to the fact that on increasing the value of Z , the presence of EDL is felt in a region farther away from the wall which enhances the viscosity, and therefore, increases the value of $C_f Re$. The variation of Nu with λ follows the same pattern as that of $C_f Re$.

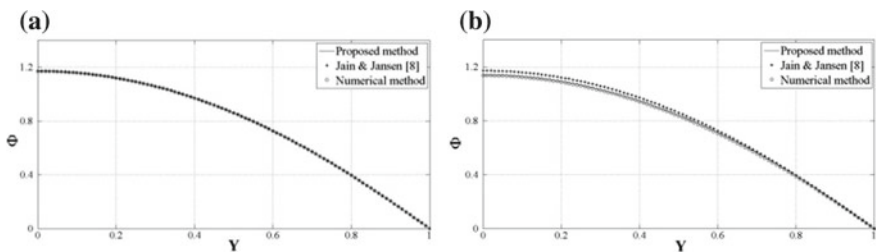


Fig. 4 Non-dimensional temperature distribution **a** $Z = 1$ and **b** $Z = 3$ for $\lambda = 10$

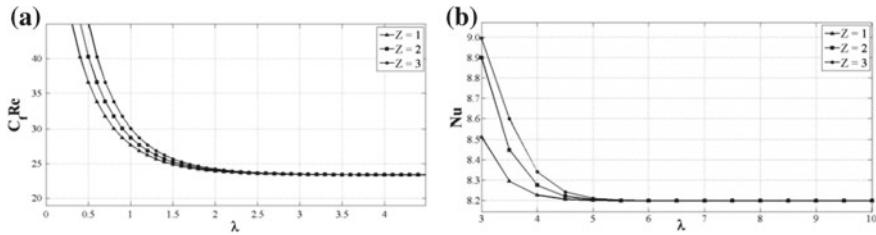


Fig. 5 Variation of **a** $C_f Re$ product and **b** Nu with λ for $Z = 1, 2,$ and 3

6 Conclusion

The present work investigates an analytical solution based on the homotopy perturbation method to analyze the characteristics of combined pressure-driven electroosmotic flow between two parallel plates. The electric potential, velocity, and temperature distributions are obtained by solving the Poisson–Boltzmann equation without Debye–Hückel approximation, the Navier–Stokes equation, and energy equation, respectively. The homotopy perturbation method is used to solve the Poisson–Boltzmann equation. Finally, the Nusselt number has been determined. The proposed results for potential, velocity, and temperature fields are presented with an existing work and numerical method for $Z = 1$ and 3 for an electrokinetic length (λ) of 10 . It is seen that the proposed method shows good agreement with the numerical method for $Z = 1$ and 3 . The Nusselt number is presented with λ for $Z = 1, 2,$ and 3 .

References

1. Coffel, J., Nuxoll, E.: BioMEMS for biosensors and closed-loop drug delivery. *Int. J. Pharm.* **544**, 335–349 (2018)
2. Wang, C., Wong, T.N., Yang, C., Ooi, K.T.: Characterization of electroosmotic flow in rectangular microchannels. *Int. J. Heat Mass Transf.* **50**, 3115–3121 (2007)
3. Drab, M., Kralj-Iglic, V.: Diffuse electric double layer in planar nanostructures due to Fermi–Dirac statistics. *Electrochim. Acta* **204**, 154–159 (2016)
4. Burgreen, D., Nakache, F.R.: Electrokinetic flow in ultrafine capillary silts. *J. Phys. Chem.* **68**, 1084–1091 (1964)
5. Khan, M., Farooq, Khan, A., W.A., Hussain, M.: Exact solution of an electroosmotic flow for generalized Burgers fluid in cylindrical domain. *Results Phys.* **6**, 933–939 (2016)
6. Ni, H., Amme, R.C.: Ion redistribution in an electric double layer. *J. Coll. Interface Sci.* **260**, 344–348 (2003)
7. Manciu, M., Manciu, F.S., Ruckenstein, E.: On the surface tension and zeta potential of electrolyte solutions. *Adv. Coll. Interface Sci.* **244**, 90–99 (2016)
8. Jain, A., Jensen, M.K.: Analytical modeling of electrokinetic effects on flow and heat transfer in microchannels. *Int. J. Heat Mass Transf.* **50**, 5161–5167 (2007)
9. Jung, Y.M., Duckjong, K., Sung, J.K.: A novel approach to analysis of electroosmotic pumping through rectangular-shaped microchannels. *Sens. Actuators B* **120**, 305–312 (2006)
10. Ngoma, G.D., Erchiqui, F.: Heat flux and slip effects on liquid flow in a microchannel. *Int. J. Therm. Sci.* **46**, 1076–1083 (2007)

11. Yıldırım, S.: Exact and numerical solutions of Poisson equation for electrostatic potential problems. *Mathematical problems in engineering* (2008)
12. Steffen, V., Silva, E.A., Evangelista, L.R., Cardozo-Filho, L.: Debye-Huckel approximation for simplification of ions adsorption equilibrium model based on Poisson-Boltzmann equation. *Surf. Interfaces* **10**, 144–148 (2018)
13. Yang, C., Li, D.Q.: Electrokinetic effects on pressure-driven liquid flows in rectangular microchannels. *J. Coll. Interf. Sci.* **194**, 95–107 (1997)
14. Kandlikar, S.G., Garimella, S., Li, D., Colin, S., King, M.R.: *Heat Transfer and Fluid Flow in Minichannels and Microchannels*. Elsevier Ltd., Great Britain (2006)